

Transient hydromagnetic three-dimensional natural convection from an inclined stretching permeable surface

Ali J. Chamkha *

Department of Mechanical and Industrial Engineering, Kuwait University, Safat 13060, Kuwait

Received 22 September 1998; received in revised form 12 September 1999; accepted 19 September 1999

Abstract

The problem of transient, laminar, three-dimensional natural convection flow over an inclined permeable surface in the presence of a magnetic field and heat generation or absorption effects is considered. The order of the governing differential equations for this investigation is reduced by using transient non-similar transformations. The resulting initial-value problem is solved numerically by an accurate, implicit, finite-difference line by line marching scheme. A parametric study is performed to illustrate the influence of the Prandtl number, Hartmann number, heat generation or absorption coefficient, and the surface suction or injection parameter on the velocity and temperature fields as well as the transient development of the skin-friction coefficients and the Nusselt number. These results are displayed graphically to show special aspects of this flow and heat transfer situation. ©2000 Elsevier Science S.A. All rights reserved.

1. Introduction

Recently, Chamkha [10] has investigated the problem of steady-state, laminar, hydromagnetic, three-dimensional free convection flow over a vertical stretching surface in the presence of heat generation or absorption effects. This was done in view of several possible metallurgical applications and processes such as annealing and tinning of copper wires, drawing of continuous filaments through quiescent fluids, extrusion of films and plates, melt spinning, glass blowing, hot rolling, manufacturing of plastic, rubber, metallic and polymer sheets, crystal growing, continuous coating and fibers spinning (see [19,33]). As mentioned by Vajravelu and Hadjinicolaou [35], the rate of cooling involved in these processes can greatly affect the properties of the end product. This rate of cooling has been shown to be controlled by the use of electrically-conducting working fluids with applied magnetic fields. The use of magnetic fields has also been applied in the process of purification of molten metals from non-metallic inclusions. Some work concerning hydro-magnetic flows and heat transfer of electrically-conducting fluids over a stretching surface can be found in the papers by Chakrabarti and Gupta [8], Chiam [15], Chandran et al. [12], and Vajravelu and Hadjinicolaou [35]. In many practical problems, the stretching of the surface can start impulsively in motion from rest with a constant or variable velocity in a stationary fluid. As a result, the velocity and

temperature fields will change with time especially at the start of the motion, thus having unsteady flow situation. The objective of this work is to consider transient hydromagnetic three-dimensional natural convection from an inclined linearly stretching porous surface in the presence of magnetic field, heat generation or absorption, and wall suction or injection effects.

Sakiadis [27,28] was the first to study boundary-layer flow over a stretched surface moving with a constant velocity. He employed a similarity transformation and obtained a numerical solution for the problem. Later, Erickson et al. [18] extended the work of Sakiadis [27,28] to account for mass transfer at the stretched sheet surface. The numerical results of Sakiadis [27,28] were confirmed experimentally by Tsuo et al. [34] for continuously moving surface with a constant velocity. In addition, Chen and Strobel [14] and Jacobi [23] have reported results for uniform motion of the stretched surface. Vajravelu and Hadjinicolaou [35] have considered hydromagnetic convective heat transfer from a stretching surface with uniform free stream and in the presence of internal heat generation or absorption effects. Many investigations have concentrated on the problem of a stretched sheet with a linear velocity and different thermal boundary conditions (see, for instance, [6,13,16,17,21,22,30,37]).

Very recently, many investigations studying the consequent flow and heat transfer characteristics that are brought about by the movement of a stretched permeable and impermeable, isothermal and non-isothermal surface with a power-law velocity variation have been reported. Banks [4]

* Corresponding author. Fax: +965-484-7131

considered the case of an impermeable wall and obtained a similarity solution. Chiam [15] considered steady flow of an electrically-conducting fluid over a surface stretching with a power-law velocity in the presence of a magnetic field. Ali [1–3] presented various extensions to Banks' [4] problem in terms of flow and thermal boundary conditions. All of the preceding references have dealt with two-dimensional flow situations. During the last decade or so, some work have been reported concerning three-dimensional and unsteady flow situations. Wang [38] considered steady-state three-dimensional flow caused by stretching flat surface. Gorla and Sidawi [20] have reported similarity transformations and numerical solutions for the problem of steady, three-dimensional free convection flow on a stretching surface with suction and blowing. Surma Devi et al. [32] have studied unsteady three-dimensional boundary-layer flow due to a stretching surface. Lakshmisha et al. [24] reported numerical solutions for three-dimensional unsteady flow with heat and mass transfer over a continuous stretching surface. Smith [29] has reported an exact solution of the unsteady Navier–Stokes equations resulting from a stretching surface. More recently, Pop and Na [26] analyzed the problem of unsteady flow past a wall which starts to stretch impulsively from rest. Chamkha [11] extended the work of Pop and Na [26] to include the thermal problem and the effects of the presence of a Darcian porous medium, magnetic field, and heat generation or absorption.

1.1. Problem formulation

Consider the transient, laminar, three-dimensional natural convective boundary-layer flow of an electrically-conducting and heat-generating/absorbing fluid over a semi-infinite inclined permeable surface stretching in the x -direction with a velocity that is linear with the distance along the surface x . Since the velocity would become very large at large x , the latter must be limited at some finite distance $x = x_a$ at which point the velocity becomes constant. The y -direction makes an angle α with the horizontal line while the z -direction is normal to the plate surface. A uniform magnetic field is applied in the y -direction. This gives rise to magnetic effects in both the x and z directions. The application of the magnetic field in the y -direction is done so as to allow suppression of convective flow in these directions. This is important in terms of controlling the quality of the product being stretched (see, [35]). In addition, uniform suction or injection is imposed at the plate surface in the z -direction. The coordinate system and flow model are shown in Fig. 1. All fluid properties are assumed constant except the density in the buoyancy terms of the x - and y -momentum equations. Assuming that the edge effects are negligible, all dependent variables will be independent of the y -direction [20]. Under the usual boundary-layer and Boussinesq approximations, the governing equations for this investigation are

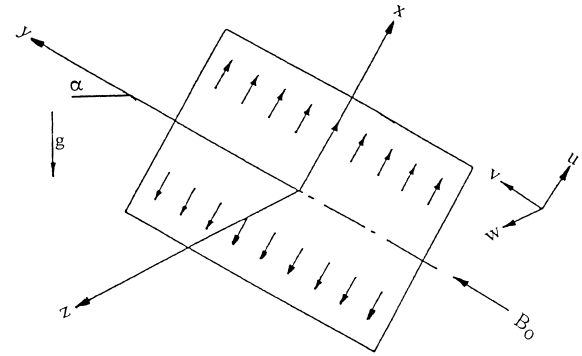


Fig. 1. Problem schematics and coordinate system.

$$\frac{\partial u}{\partial x} + \frac{\partial w}{\partial z} = 0 \quad (1)$$

$$\begin{aligned} \frac{\partial u}{\partial t} + u \frac{\partial u}{\partial x} + w \frac{\partial u}{\partial z} \\ = \nu \frac{\partial^2 u}{\partial z^2} + g\beta (T - T_\infty) \cos \alpha - \frac{\sigma}{\rho} B_0^2 u \end{aligned} \quad (2)$$

$$\frac{\partial v}{\partial t} + w \frac{\partial v}{\partial z} = \nu \frac{\partial^2 v}{\partial z^2} + g\beta (T - T_\infty) \sin \alpha \quad (3)$$

$$\frac{\partial w}{\partial t} + w \frac{\partial w}{\partial z} = -\frac{1}{\rho} \frac{\partial p}{\partial z} + \nu \frac{\partial^2 w}{\partial z^2} - \frac{\sigma B_0^2}{\rho} w \quad (4)$$

$$\frac{\partial T}{\partial t} + w \frac{\partial T}{\partial z} = \frac{\nu}{\text{Pr}} \frac{\partial^2 T}{\partial z^2} + \frac{Q_0}{\rho c_p} (T - T_\infty) \quad (5)$$

where x , y , and z are the coordinates directions. u , v , w , p , and T are the fluid velocity components in the x , y , and z directions, pressure and temperature, respectively. ρ , ν , c_p and Pr are the fluid density, kinematic viscosity, specific heat at constant pressure, and the Prandtl number, respectively. g , β , T_∞ and α are the gravitational acceleration, coefficient of thermal expansion, ambient temperature, and the inclination angle, respectively. σ , B_0 , and Q_0 are the fluid electrical conductivity, magnetic induction, and dimensional heat generation/absorption coefficient, respectively. It should be noted that in writing Eqs. (1)–(5), the magnetic Reynolds number is assumed small so that the induced magnetic field is neglected. Also, the Hall effect of magnetohydrodynamics, Joule heating, and the viscous dissipation are neglected. In many physical situations such as crystal growing, the heat generation or absorption effects in the fluid are greatly dependent on temperature. Sparrow and Cess [31], Moalem [25], Vajravelu and Nayfeh [36], Chamkha [9], and Vajravelu and Hadjinicolaou [35] have considered temperature-dependent heat generation (source) or absorption (sink). Following these authors, the heat generation or absorption term (last term) of Eq. (5) is assumed to vary linearly with the difference of the fluid temperature in the boundary layer and the ambient temperature at $z = \infty$.

The appropriate boundary conditions for this problem can be written as

$$\begin{aligned}
 u(t, x, 0) &= bx, & v(t, x, 0) &= 0, & w(t, x, 0) &= w_0, \\
 T(t, x, 0) &= T_w & u(t, x, \infty) &= 0, & v(t, x, \infty) &= 0, \\
 \frac{\partial w}{\partial z}(t, x, 0) &= 0, & T(t, x, \infty) &= T_\infty
 \end{aligned} \tag{6}$$

where w_0 and T_w are the wall suction or injection velocity and temperature, respectively.

In order to minimize the numerical efforts to solve the governing equations, the following transformations are introduced:

$$\begin{aligned}
 \tau &= t, & \eta &= \frac{z}{\sqrt{\nu t}}, & u &= bx\phi'(\tau, \eta) + \Gamma \cos \alpha M(\tau, \eta), \\
 v &= T \sin \alpha N(\tau, \eta), & w &= -\sqrt{b^2 \nu t} \phi, \\
 p &= \rho b \nu G(\tau, \eta), & \theta(\tau, \eta) &= \frac{T - T_\infty}{T_w - T_\infty}, \\
 \Gamma &= \frac{g\beta(T_w - T_\infty)}{b}
 \end{aligned} \tag{7}$$

Substituting Eq. (7) into Eqs. (1)–(6) reduces the number of independent variables by one and produces the following non-similar transient equations:

$$\phi''' + \frac{\eta}{2} \phi'' + b\tau(\phi \phi'' - (\phi')^2 - Ha^2 \phi') - \tau \frac{\partial \phi'}{\partial \tau} = 0 \tag{8}$$

$$\begin{aligned}
 M'' + \frac{\eta}{2} M' + b\tau(\phi M' - \phi' M - Ha^2 M + \theta) \\
 - \tau \frac{\partial M}{\partial \tau} = 0
 \end{aligned} \tag{9}$$

$$N'' + \frac{\eta}{2} N' + b\tau(\phi N' + \theta) - \tau \frac{\partial N}{\partial \tau} = 0 \tag{10}$$

$$G' + \phi'' + \frac{\eta}{2} \phi' - \frac{\phi}{2} + b\tau(\phi \phi' - Ha^2 \phi) - \tau \frac{\partial \phi}{\partial \tau} = 0 \tag{11}$$

$$\theta'' + \text{Pr} \frac{\eta}{2} \theta' + \text{Pr} b\tau(\phi \theta' + \gamma \theta) - \text{Pr} \tau \frac{\partial \theta}{\partial \tau} = 0 \tag{12}$$

where a prime denotes partial differentiation with respect to η and $Ha^2 = \sigma B_0^2 / (\rho b)$, $\gamma = Q_o / (\rho c_p b)$ and $\phi_w = -w_0 / \sqrt{b\nu}$ are the square of the magnetic Hartmann number, the dimensionless heat generation/absorption coefficient, and the wall mass transfer coefficient, respectively. It should be noted that positive values of ϕ_w indicate fluid suction at the plate surface while negative values of ϕ_w indicate fluid blowing or injection at the wall. In addition, it is seen that the advantage of employing the transformations (7) is that they reduce the number of independent variables by one and that similarity equations are obtained at $\tau = 0$. In this way, the initial profiles or conditions for ϕ , ϕ' , M , N , G , and θ are obtained by solving these similar equations subject to the boundary conditions.

The transformed boundary conditions become

$$\begin{aligned}
 \phi(\tau, 0) &= \phi'(\tau, 0) = 1, & \phi'(\tau, \infty) &= 0 \\
 M(\tau, 0) &= 0, & M(\tau, \infty) &= 0, & N(\tau, 0) &= 0, & N(\tau, \infty) &= 0 \\
 G(\tau, 0) &= 0, & \phi(\tau, 0) &= 1, & \theta(\tau, \infty) &= 0
 \end{aligned} \tag{13}$$

Important physical parameters for this flow and heat transfer situation are the skin-friction coefficients in the x and y directions and the local Nusselt number. The shear stresses at the stretching surface in both the x and y directions, respectively, are given by

$$\begin{aligned}
 \tau_{zx} &= \mu \frac{\partial u}{\partial z}(t, x, 0) \\
 &= \frac{\mu}{\sqrt{\nu t}} (bx \phi''(\tau, 0) + \Gamma \cos \alpha M'(\tau, 0))
 \end{aligned} \tag{14}$$

$$\tau_{zy} = \mu \frac{\partial v}{\partial z}(t, x, 0) = \frac{\mu}{\sqrt{\nu t}} \Gamma \sin \alpha N'(\tau, 0) \tag{15}$$

where $\mu (= \rho \nu)$ is the dynamic viscosity of the fluid. The corresponding skin-friction coefficients in the x and y directions are obtained, respectively, by dividing Eqs. (14) and (15) by the quantity $\rho(bx)^2/2$ which represents the dynamic pressure to yield

$$C_{fx} = \frac{2x}{\text{Re}_x \sqrt{\nu t}} \left(\frac{\text{Gr}_x}{\text{Re}_x^2} \cos \alpha M'(\tau, 0) + \phi''(\tau, 0) \right) \tag{16}$$

$$C_{fy} = \frac{2x}{\text{Re}_x \sqrt{\nu t}} \left(\frac{\text{Gr}_x}{\text{Re}_x^2} \right) \sin \alpha N'(\tau, 0) \tag{17}$$

where $\text{Gr}_x = g\beta(T_w - T_\infty)x^3/\nu^2$ and $\text{Re}_x = bx^2/\nu$ are the local Grashof and Reynolds numbers, respectively.

The wall heat transfer is given by Fourier's law of conduction as follows

$$q_w = -k \frac{\partial T}{\partial z}(t, x, 0) = -\frac{k}{\sqrt{\nu t}} (T_w - T_\infty) \theta'(\tau, 0) \tag{18}$$

where k is the thermal conductivity of the fluid. The local Nusselt number for this situation can then be defined as

$$Nu_x = \frac{h x}{k} = \frac{q_w x}{k(T_w - T_\infty)} = -\frac{x}{\sqrt{\nu t}} \theta'(\tau, 0) \tag{19}$$

where h is the local heat transfer coefficient.

1.2. Numerical scheme

Eqs. (8)–(13) represent an initial-value problem in which the initial profiles for ϕ' , M , N , G , and θ are obtained directly by solving the similarity equations obtained by setting $\tau = 0$ in these equations subject to the boundary conditions. Once the initial profiles are obtained, a forward marching technique in τ can be used to obtain the solutions for all of the dependent variables at different times. The implicit finite-difference method discussed by Blottner [5] which is similar to the Keller's box method (see [7]) have proven to be successful for the solution of similar and non-similar boundary-layer equations. For this reason, it is adopted for the solution of the present investigation.

Non-uniform grid distributions in both the η and τ directions with small initial step sizes were used to accommodate steep changes in the velocity and temperature gradients in

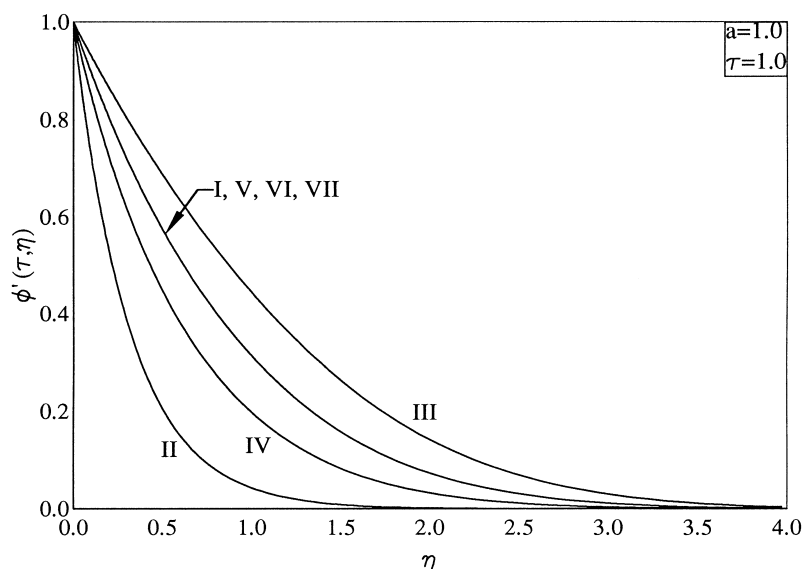


Fig. 2. Effects of Ha , ϕ_w , γ and Pr on $\phi'(1, \eta)$.

the immediate vicinity of the wall and at the start of the flow. The initial step size employed in the η direction was $\Delta\eta_1 = 0.001$ and the growth factor was $K_1 = 1.03$ such that $\Delta\eta_{i+1} = K_1 \Delta\eta_i$ while an initial step size $\Delta\tau_1 = 0.001$ and a growth factor $K_2 = 1.03$ such that $\Delta\tau_{j+1} = K_2 \Delta\tau_j$ were used in the τ direction. A computational domain consisting of 196 grid points in the η direction and 171 grid points in the τ direction was utilized. This gave $\eta_\infty \approx 10$ and $\tau_\infty \approx 5$. The independence of the results from the grid density was ensured and successfully checked by various trial and error numerical experimentations.

All first-order derivatives in τ are replaced by two-point backward-difference formulae. Then, Eq. (8) was converted into a second-order ordinary differential equation by letting $F = \phi'$. Then, the resulting equation in F along with Eqs. (9)–(11) were discretized using three-point central difference quotients while the equation $\phi' - F = 0$ and Eq. (12) were discretized by the trapezoidal rule. Linearization of the equations was performed by evaluation of the non-linear terms at the previous iteration. At each line of constant τ , linear tri-diagonal algebraic equations resulted which were solved by the Thomas algorithm (see, [5]). The convergence criterion required that the difference between the current and the previous iterations be 10^{-5} . When this condition was satisfied, the solution was assumed converged and the iteration process was terminated.

Comparisons with the works of Pop and Na [26] and Chamkha [11] for unsteady flow over a stretching sheet were conducted and the results were found to be in excellent agreement. It should be mentioned that these comparisons required slight changes in the coefficients of Eqs. (8) and (12) to make them similar to those reported by Pop and Na [26] and Chamkha [11]. These favorable comparisons lend some confidence to the accuracy of the numerical method.

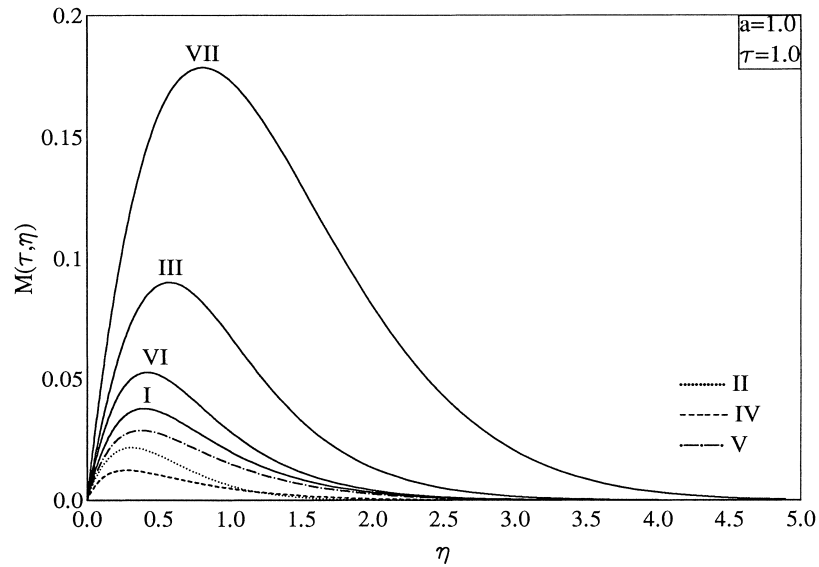
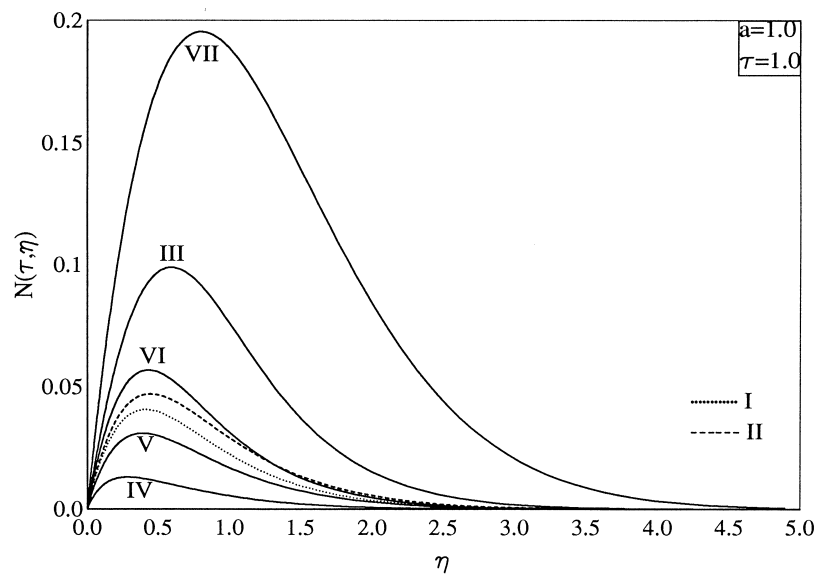
Table 1

Parametric values for the curves used in the figures

Curve	Ha	Pr	γ	ϕ_w
I	0.0	6.7	0.0	0.0
II	3.0	6.7	0.0	0.0
III	0.0	6.7	0.0	-1.0
IV	0.0	6.7	0.0	1.0
V	0.0	6.7	-1.0	0.0
VI	0.0	6.7	1.0	0.0
VII	0.0	0.7	0.0	0.0

2. Results and discussion

Figs. 2–7 display the effects of all of the Hartmann number Ha , the suction or injection parameter ϕ_w , the heat generation or absorption coefficient γ and the fluid's Prandtl number Pr on the profiles of $\phi'(\tau, \eta)$, $M(\tau, \eta)$, $N(\tau, \eta)$, $\phi(\tau, \eta)$, $G(\tau, \eta)$, and $\theta(\tau, \eta)$ at $\tau = 1$, respectively. In these and all subsequent figures, the parametric conditions associated with each of the curves present are given in Table 1. The parametric study of the physical parameters involved in the problem is done this way so as to minimize the number of figures needed for this purpose. It should be noted that, for the reference case (Curve I), water electrolyzed with a little of acid ($Pr = 6.7$) is used as the working fluid. Application of a magnetic field in the y direction to an electrically-conducting fluid gives rise to a flow resistive force called the Lorentz force. This force will have components in both the x and z directions. This causes both parts of x -velocity component ϕ' and M as well as the z -component of velocity ϕ to decrease. However, the velocity component in the y direction N , the fluid pressure G and the fluid temperature tend to increase due to the presence of the magnetic field. Also, imposition of fluid suction at the stretching surface has the tendency to reduce both the hydrodynamic and thermal boundary layers close to the wall.

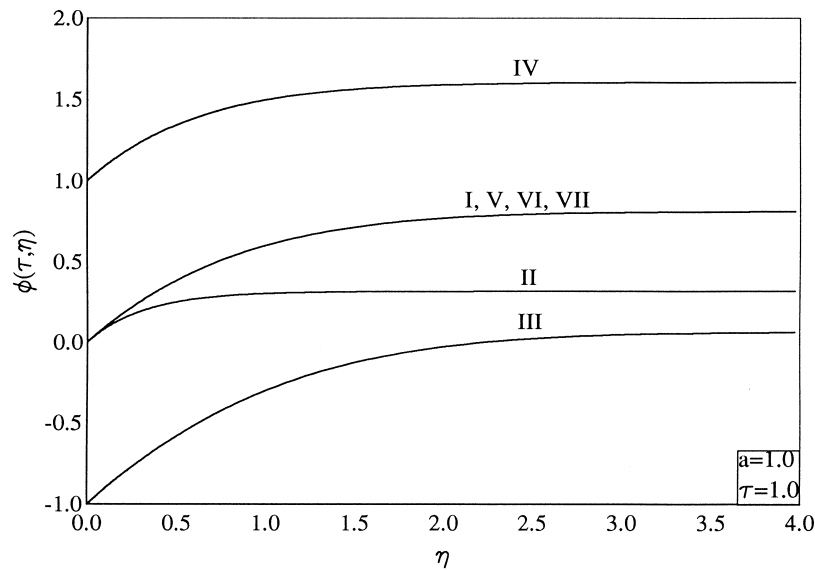
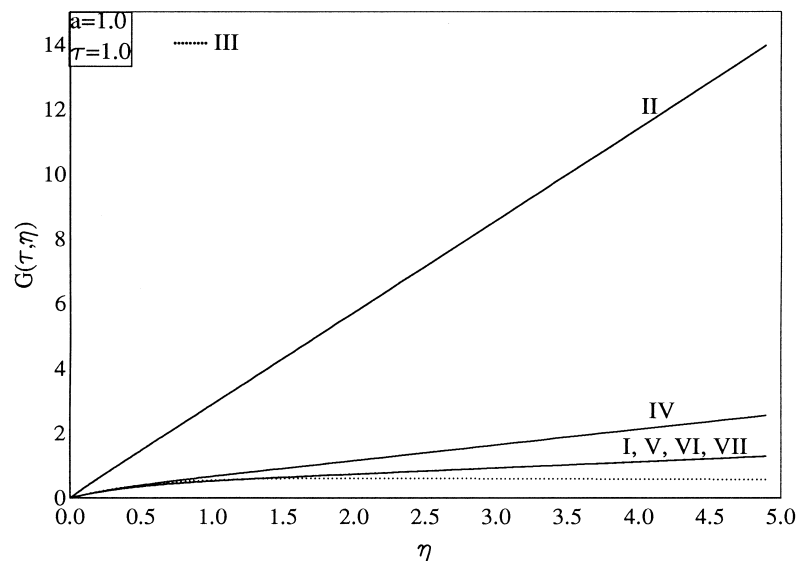
Fig. 3. Effects of Ha , ϕ_w , γ and Pr on $M(1,\eta)$.Fig. 4. Effects of Ha , ϕ_w , γ and Pr on $N(1,\eta)$.

This will produce lower flow velocities and temperatures and higher fluid pressures. However, injecting or blowing fluid into the boundary layer through the surface of the plate produces the opposite effect, namely, higher flow velocities and temperatures and lower fluid pressures. It should be mentioned here that injection of fluid into the boundary layer must occur in limited amounts so as not to destroy the natural convection phenomenon.

Obviously, the presence of a heat generation mechanism causes the fluid temperature θ to increase. This increase in temperature is translated into increased thermal buoyancy-induced flow along the surface. On the other hand, heat absorption effects yield lower fluid temperatures

and, therefore, lower flow velocities along the plate. It should be noted that Eqs. (8) and (11) governing ϕ' , ϕ and G are uncoupled from the other equations and, therefore, are unaffected by changes in the heat generation or absorption coefficient γ . In contrast with the heat generation effect, increases in the fluid's Prandtl number result in lower temperature distributions and, therefore, reduced thermal buoyancy-induced flow along the stretching surface. Again, the profiles of ϕ' , ϕ and G are unchanged by changes in Pr for the same reason mentioned above. All of the above mentioned behaviors are clear from Figs. 2–7.

Figs. 8–11 depict the transient changes in the wall slopes of ϕ' , M , N , and θ as a result of changing any of the physical

Fig. 5. Effects of Ha ϕ_w , γ and Pr on $\phi(1,\eta)$.Fig. 6. Effects of Ha ϕ_w , γ and Pr on $G(1,\eta)$.

parameters Ha, ϕ_w , γ and Pr, respectively. As indicated before, increases in the Hartmann number Ha has a tendency to decrease the flow velocities in the x and z directions and to increase the y -component of velocity and temperature. This flow retardation effect in the x direction causes lower shear stresses at the stretching surface represented by decreases in the values of $\phi''(\tau, 0)$ and $M'(\tau, 0)$ at any time. However, the acceleration of flow in the y direction resulting from increasing Ha produces higher shear stresses in the y direction represented by the increases in $N'(\tau, 0)$. Also, the increases in the temperature profile due to increases in Ha result in higher wall temperature slopes. Therefore, the wall heat transfer represented by $-\theta'(\tau, 0)$ decreases. The lower

flow velocities and temperatures resulting from application of fluid suction at the surface are followed by decreases in the wall slopes of ϕ' , M , N , and θ (or higher $\theta'(\tau, 0)$ values) at every time. However, the opposite effect is obtained for wall fluid blowing or injection. It should be noted that the wall heat transfer $-\theta'(\tau, 0)$ is more responsive to suction than injection as it increases sharply with time as is clear from Fig. 11. As mentioned before, changes in either of the heat generation or absorption coefficient γ or the Prandtl number Pr produce no changes in the profiles of $\phi(\tau, \eta)$ and, therefore, no variations in the values of $\phi''(\tau, 0)$. As seen before, the physical effect of heat generation ($\gamma > 0$) is the same as decreasing the fluid's Prandtl number since

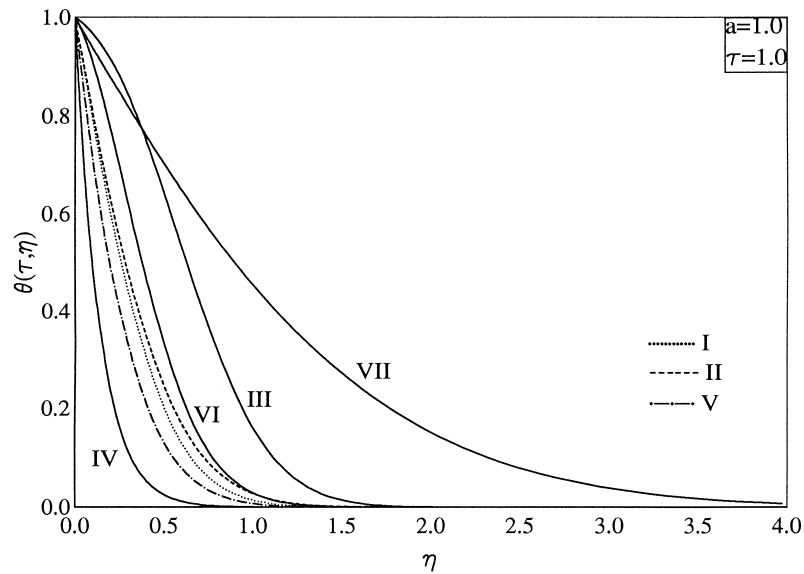


Fig. 7. Effects of Ha , ϕ_w , γ and Pr on $\theta(1,\eta)$.

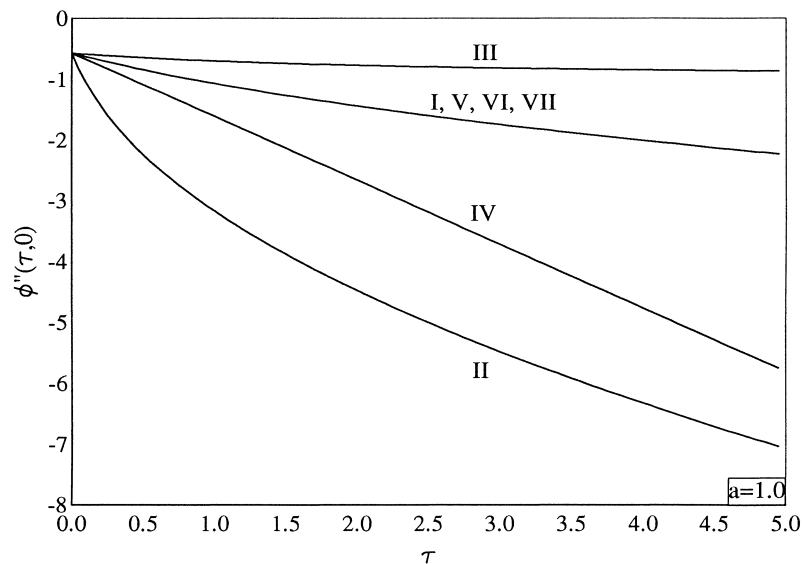


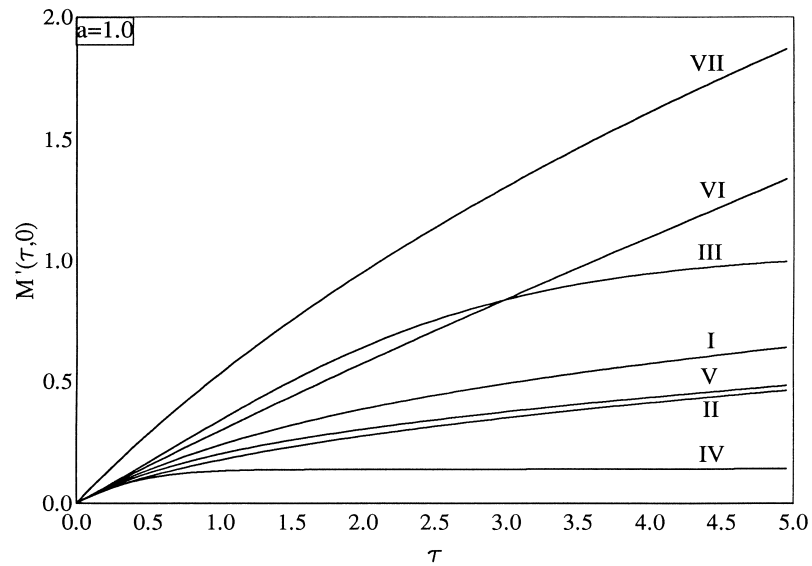
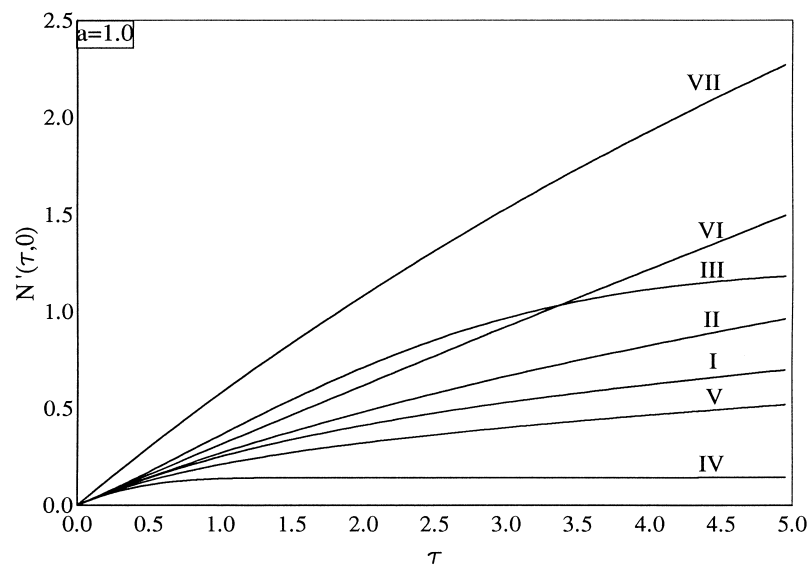
Fig. 8. Effects of Ha , ϕ_w , γ and Pr on $\phi''(\tau,0)$.

both situations produce higher flow temperatures and thermal buoyancy-induced flow. Thus, in both situations, the values of $M'(\tau,0)$, $N'(\tau,0)$ and $-\theta'(\tau,0)$ increase indicating higher wall shear stresses in the x and y directions and lower wall heat transfer ($-\theta'(\tau,0)$). On the other hand, heat absorption obtains the opposite effect which is reduced wall shear stresses and higher wall heat transfer. All of the behaviors discussed above are clearly illustrated in Figs. 8–11.

3. Conclusion

The problem of transient, laminar, natural convection boundary-layer flow of an electrically-conducting fluid

along an inclined porous surface stretching with a linear velocity in the presence of a magnetic field, heat generation or absorption, and fluid wall suction or injection effects was investigated numerically. A new transformation was introduced in which the governing unsteady three-dimensional equations were transformed into non-similar equations. By using this transformation, the number of independent variables was reduced by one. The resulting equations produced their own initial conditions by solving the similarity equations obtained at $\tau=0$. The numerical solution was obtained by an implicit, iterative, finite-difference marching technique. The accuracy of the numerical method was tested by comparison of a special case of this problem with previously published work. Numerical results for the ve-

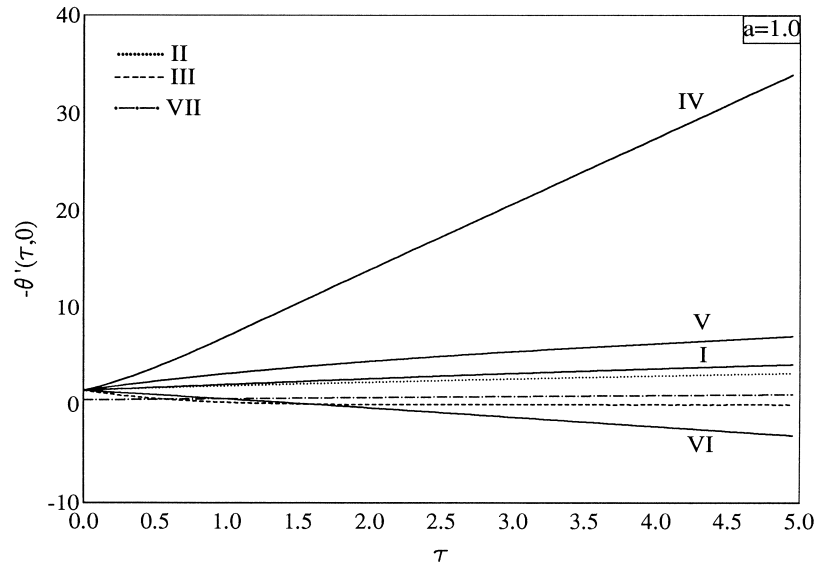
Fig. 9. Effects of Ha , ϕ_w , γ and Pr on $M'(\tau,0)$.Fig. 10. Effects of Ha , ϕ_w , γ and Pr on $N'(\tau,0)$.

locity and temperature profiles were presented graphically for various parametric conditions. In addition, the transient development of the wall slopes for the velocity and thermal functions were also displayed for different values of the wall suction or injection parameter, Prandtl number, Hartmann number, and the dimensionless heat generation/absorption coefficient. It was found that imposition of fluid wall suction increased the transient wall heat transfer distribution and decreased the time history of the skin-friction coefficients in both the x and y directions. The same was observed as the fluid Prandtl number was increased. In addition, the opposite result was obtained as the dimensionless heat generation coefficient was increased, namely, higher skin-friction coefficients and lower wall heat transfer time histories. However, the effect of the magnetic field was found to be

decreasing the wall heat transfer and the skin-friction coefficient in the x direction while increasing the skin-friction coefficient in the y direction at any time. It is hoped that the numerical results presented in this paper will be used for validation of other studies on unsteady flow and heat transfer from a stretching surface.

4. Nomenclature

b	a constant having units of inverse time
B_0	magnetic induction
c_p	fluid specific heat at constant pressure
C_{fx}	skin-friction coefficient in the x direction
C_{fy}	skin-friction coefficient in the y direction

Fig. 11. Effects of Ha , ϕ_w , γ and Pr on $\theta'(\tau, \eta)$.

g	acceleration due to gravity
G	dimensionless pressure
Gr_x	local Grashof number
h	local heat transfer coefficient
Ha	magnetic Hartmann number
k	fluid thermal conductivity
M	function related to dimensionless x -component of velocity
N	dimensionless y -component of velocity
Nu_x	local Nusselt number
p	pressure
Pr	Prandtl number
q_w	wall heat transfer
Q_0	heat generation/absorption coefficient
Re_x	local Reynolds number
t	time
T	temperature
u	x -component of velocity
v	y -component of velocity
w	z -component of velocity
w_0	wall suction or injection velocity
x, y, z	coordinate system directions

4.1. Greek symbols

α	surface inclination angle
β	thermal expansion coefficient
η	transformed variable combining t and z
ϕ	dimensionless z -component of velocity
γ	dimensionless heat generation/absorption coefficient
Γ	constant defined in Eq. (7)
μ	fluid dynamic viscosity
ν	fluid kinematic viscosity
ρ	fluid density

σ	fluid electrical conductivity
τ	time
τ_{zx}	shear stress in the x direction
τ_{zy}	shear stress in the y direction
θ	dimensionless temperature

4.2. Subscript

w	wall
∞	ambient

References

- [1] M.E. Ali, Heat transfer characteristics of a continuous stretching surface, *Warme und Stoffübertragung* 29 (1994) 227–234.
- [2] M.E. Ali, On thermal boundary layer on a power-law stretched surface with suction or injection, *Int. J. Heat and Fluid Flow* 16 (1995) 280–290.
- [3] M.E. Ali, The effect of suction or injection on the laminar boundary layer development over a stretched surface, *J. King Saud Univ. Eng. Sci.* No. 1 (1996) 8, in press.
- [4] W.H.H. Banks, Similarity solutions of the boundary-layer equations for a stretching wall, *J. Mécanique Théorique et Appliquée* 2 (1983) 375–392.
- [5] F.G. Blottner, Finite-difference methods of solution of the boundary-layer equations, *AIAA J.* 8 (1970) 193–205.
- [6] P. Carragher, L.J. Crane, Heat transfer on a continuous stretching sheet, *ZAMM* 62 (1982) 564–565.
- [7] T. Cebeci, P. Bradshaw, *Momentum Transfer in Boundary Layers*, Hemisphere, Washington, DC, 1977.
- [8] A. Chakrabarti, A.S. Gupta, Hydromagnetic flow and heat transfer over a stretching sheet, *Q. Appl. Math.* 37 (1979) 73–78.
- [9] A.J. Chamkha, Non-Darcy hydromagnetic free convection from a cone and a wedge in porous media, *Int. Commun. Heat Mass Transfer* 23 (1996) 875–887.
- [10] A.J. Chamkha, Hydromagnetic three-dimensional free convection on a vertical stretching surface with heat generation or absorption, *Int. J. Heat Fluid Flow* (1998), in press.

- [11] A.J. Chamkha, Unsteady hydromagnetic flow and heat transfer from a non-isothermal stretching surface immersed in a porous medium, *Int. Commun. Heat Mass Transfer*, 1998, in press.
- [12] P. Chandran, N.C. Sacheti, A.K. Singh, Hydromagnetic flow and heat transfer past a continuously moving porous boundary, *Int. Commun. Heat Mass Transfer* 23 (1996) 889–898.
- [13] C.K. Chen, M. Char, Heat transfer of a continuous stretching surface with suction or blowing, *J. Math. Anal. Appl.* 135 (1988) 568–580.
- [14] T.S. Chen, F.A. Strobel, Buoyancy effects in boundary layer adjacent to a continuous moving horizontal flat plate, *J. Heat Transfer* 102 (1980) 170–172.
- [15] T.C. Chiam, Hydromagnetic flow over a surface stretching with a power-law velocity, *Int. J. Eng. Sci.* 33 (1995) 429–435.
- [16] L.J. Crane, Flow past a stretching plane, *Z. Angew. Math. Phys.* 21 (1970) 645–647.
- [17] B.K. Dutta, A.S. Gupta, Cooling of a stretching sheet in a viscous flow with suction or blowing, *ZAMM* 68 (1988) 231–236.
- [18] L.E. Erickson, L.T. Fan, V.G. Fox, Heat and mass transfer on a moving continuous flat plate with suction or injection, *Ind. Eng. Chem.* 5 (1966) 19–25.
- [19] E.G. Fisher, *Extrusion of Plastics*, Wiley New York, 1976.
- [20] R.S.R. Gorla, I. Sidawi, Free convection on a vertical stretching surface with suction and blowing, *Appl. Sci. Res.* 52 (1994) 247–257.
- [21] L.G. Grubka, K.M. Bobba, Heat transfer characteristics of a continuous stretching surface with variable temperature, *J. Heat Transfer* 107 (1985) 248–250.
- [22] P.S. Gupta, A.S. Gupta, Heat and mass transfer on a stretching sheet with suction or blowing, *Can. J. Chem. Eng.* 55(6) (1977) 744–746.
- [23] A.M. Jacobi, A scale analysis approach to the correlation of continuous moving sheet (backward boundary layer) forced convective heat transfer, *J. Heat Transfer* 115 (1993) 1058–1061.
- [24] K.N. Lakshmisha, S. Venkateswaran, G. Nath, Three-dimensional unsteady flow with heat and mass transfer over a continuous stretching surface, *J. Heat Transfer* 110 (1988) 590–595.
- [25] D. Moalem, Steady-state heat transfer within porous medium with temperature dependent heat generation, *Int. J. Heat Mass Transfer* 19 (1976) 529–537.
- [26] I. Pop, T.-Y. Na, Unsteady flow past a stretching sheet, *Mech. Res. Commun.* 23 (1996) 413–422.
- [27] B.C. Sakiadis, Boundary-layer behavior on continuous solid surfaces I. Boundary-layer equations for two-dimensional and axisymmetric flow, *AIChE Journal* 7(1) (1961) 26–28.
- [28] B.C. Sakiadis, Boundary-layer behavior on continuous solid surface: II. Boundary-layer on a continuous flat surface, *AIChE J.* 7(1) (1961) 221–225.
- [29] S.H. Smith, An exact solution of the unsteady Navier–Stokes equations resulting from a stretching surface, *ASME J. Appl. Mech.* 61 (1994) 629–633.
- [30] V.M. Soundalgekar, T.V. Ramana Murty, Heat transfer past a continuous moving plate with variable temperature, *Warme und Stoffübertragung* 14 (1980) 91–93.
- [31] E.M. Sparrow, R.D. Cess, Temperature-dependent heat sources or sinks in a stagnation point flow, *Appl. Sci. Res.* A10 (1961) 185–197.
- [32] C.D. Surma Devi, H.S. Takhar, G. Nath, Unsteady three-dimensional boundary layer flow due to a stretching surface, *Int. J. Heat and Mass Transfer* 29 (1986) 1996–1999.
- [33] Z. Tadmor, I. Klein, *Engineering Principles of Plasticating Extrusion*, Polymer Science and Engineering Series, Van Nostrand Reinhold, New York, 1970.
- [34] F.K. Tsou, E.M. Sparrow, R.J. Goldstein, Flow and heat transfer in the boundary layer on a continuous moving surface, *Int. J. Heat and Mass Transfer* 10 (1967) 219–235.
- [35] K. Vajravelu, A. Hadjinicolaou, Convective heat transfer in an electrically conducting fluid at a stretching surface with uniform free stream, *Int. J. Eng. Sci.* 35 (1997) 1237–1244.
- [36] K. Vajravelu, J. Nayfeh, Hydromagnetic convection at a cone and a wedge, *Int. Commun. Heat Mass Transfer* 19 (1992) 701–710.
- [37] J. Vlegaar, Laminar boundary-layer behavior on continuous, accelerating surfaces, *Chem. Eng. Sci.* 32 (1977) 1517–1525.
- [38] C.Y. Wang, The three-dimensional flow due to a stretching flat surface, *Phys. of Fluids* 27 (1984) 1915–1917.